A 16 Element Quasi-Optical FET Oscillator Power Combining Array with External Injection Locking

Joel Birkeland, *Member, IEEE,* and Tatsuo Itoh, *Fellow, IEEE*

Abstract—**In this paper we present analysis, design and experimental results of a 16 element planar oscillator array for quasi-optical power combining. Each element in the array consists of a single FET oscillator with an input port for injection of the locking signal, and an output port which is connected to a patch radiator. The array is synchronized using a 16 way power dividing network which distributes the locking signal to the oscillating elements. The array is constructed using a two-sided microstrip configuration, with the oscillators and feed network on one side of a ground plane, and the patch radiators on the opposite side. An effective radiated power (ERP) of 28.2 W CW with an isotropic conversion gain (G_{iso}) of 9.9 dB was measured at 6 GHz. For an injected power of 10.3 dBm, a locking range of 453 MHz at a center frequency of 6.014 GHz was obtained; a bandwidth of 7.5%. Because of the simple nature of the individual oscillator elements, this approach is well suited to MMIC implementation.**

I. Introduction

SOLID-STATE sources of microwave and millimeter wave energy have several well-known advantages over tubes, including size and lifetime. At millimeter-wave frequencies, however, solid state sources are not currently available with output powers comparable to tube sources. For this reason, the generation of high power levels using solid state devices requires the combination of the outputs of many individual sources [1].

A recent approach to power combining which appears particularly well suited to solid-state millimeter-wave applications is quasi-optical power combining [2]. In this method, the individual solid state devices are arrayed on a plane, and each is provided with some means of coupling to a radiated field. When the sources are synchronized, the radiated fields are combined in free space above the array. This approach eliminates the loss associated with guided-wave type combining networks. Gunn diode or FET oscillators coupled to patch radiators have been investigated for this purpose [3]–[7]. A similar approach involves a grid of FETs positioned in a Fabry–Perot cavity [8]. The oscillators are synchronized by the weak coupling between the radiating elements. In some cases dielectric reflecting elements are used to provide feedback to sustain the oscillations [6], [8].

The ability to injection lock microwave oscillators greatly enhances their usefulness [9]. In addition to the important function of stabilization, an injection locked oscillator can be used as an FM amplifier. In this case, the injection locked oscillator may realize much greater gain than a comparable amplifier, albeit over a narrower bandwidth. For the oscillator arrays described in the references given above, the appropriate method is spatial injection locking, which is achieved by illuminating the array with a plane wave injection source. One consequence of this approach is that for maximum locking bandwidth, the injection source must be placed in the direction of the main beam [8]. Also, in order to illuminate the radiating elements with an approximately equi-phase injection field, it may necessary to place the source quite a distance away from the array, thereby necessitating a high power injection source. Given these considerations, it is uncertain whether this type of injection locking is practical.

In this paper, a new type of power combining array is presented, using two-port FET oscillators as the active elements [10]. The two-port oscillators are arranged in a square planar array, with the output of each connected to a patch radiator. The key difference between this approach and previous work is that in this method, the oscillators are individually injection locked to a single external source by means of a Wilkinson-type 16 way power divider, rather than by parasitic coupling between the radiating elements. This is made possible by the design of the oscillator element, which features a separate injection port. Because of the properties of this type of oscillator, the injection locking range for the array is quite broad.

II. Analysis of the Oscillator Element

A circuit diagram of the oscillator element used in the array is shown in Fig. 1. The circuit consists of a single FET amplifier, with a pair of microstrip coupled lines providing feedback. The injection source and load impedance complete the circuit. The voltage associated with the load is included to allow the possibility of any stray signal coupled in at this port. A brief description of this circuit appears in [10]; a more detailed analysis is given here.

Manuscript received May 13, 1991; revised August 29, 1991. This work was supported by the U.S. Army Research Office under contract DAAL03-88-K-0005.

J. Birkeland is with Motorola Semiconductor Product Sector, EL609, 2100 East Eliott Road, Tempe, AZ 85284.

T. Itoh is with the Department of Electrical Engineering, University of California, Los Angeles, CA 90024-1594.

IEEE Log Number 9105452.

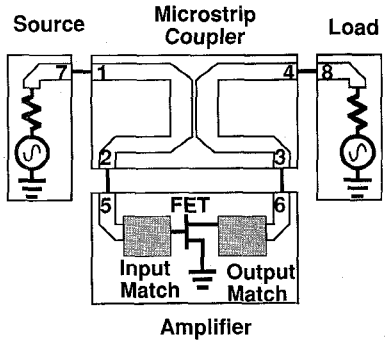

Fig. 1. Schematic diagram of feedback oscillator, showing port numbering.

A. Oscillation Condition

The technique used here to determine the oscillation conditions of a microwave network is based on the connection-scattering method given in [11]. In the following discussion, some of the scattering parameters of the networks are allowed to be functions of the wave amplitudes as well as frequencies. In this case, we neglect any harmonics generated by the nonlinear behavior, and we define the scattering parameters to be the ratio of the fundamental components of the incident and scattered waves.

Following the procedure given in the above reference for the analysis of an arbitrarily connected microwave network, we construct a block diagonal matrix $\boldsymbol{S}^{\text{tot}}$, whose elements are the scattering matrices of the individual circuit components, e.g.:

$$\boldsymbol{S}^{\text{tot}} = \begin{vmatrix} \boldsymbol{S}^1 & & 0 \\ & \boldsymbol{S}^2 & \\ 0 & & \ddots \end{vmatrix}$$

where $\boldsymbol{S}^i$ is a minor matrix which is the scattering matrix for the ith circuit element, etc. . . . For the circuit shown in Fig. 1, for example $\boldsymbol{S}^{\text{tot}}$ is given by

$$\boldsymbol{S}^{\text{tot}} = \begin{vmatrix} \boldsymbol{S}^{\text{cplr}} & & 0 & 0 \\ & \boldsymbol{S}^{\text{amp}} & & 0 \\ 0 & & \Gamma_{\text{inj}} & \\ 0 & 0 & & \Gamma_{\text{pat}} \end{vmatrix},$$

where $\boldsymbol{S}^{\text{cplr}}$ is the 4×4 scattering matrix associated with the coupled lines, $\boldsymbol{S}^{\text{amp}}$ is the 2×2 scattering matrix of the FET amplifier, and Γ_{inj} and Γ_{pat} are the reflection coefficients of the injection source and patch antenna, respectively. The port numbering in Fig. 1 is consistent with this formulation. For a single oscillator in free-running mode, the source and load voltages are zero, and the governing relations for all of the components may be written as

$$\boldsymbol{b} = \boldsymbol{S}^{\text{tot}}\boldsymbol{a}, \tag{1}$$

where $\boldsymbol{a}$ and $\boldsymbol{b}$ represent the incident and scattered wave vectors, respectively.

Equation (1) does not take into account the constraints imposed by the interconnections between the components. For example, from Fig. 1, it is clear that $a_7 = b_1$ and $a_1 = b_7$; similarly for the other ports. The matrix $\boldsymbol{G}$ is introduced to account for these constraints. $\boldsymbol{G}$ has the same order as $\boldsymbol{S}^{\text{tot}}$, with the i, jth element equal to 1 if ports i and j in the network are connected, and 0 otherwise:

$$\boldsymbol{b} = \boldsymbol{G}\boldsymbol{a}. \tag{2}$$

Combining (1) and (2) gives

$$(\boldsymbol{S}^{\text{tot}} - \boldsymbol{G})\boldsymbol{a} = 0. \tag{3}$$

The frequencies and amplitudes of the possible oscillations are given by the roots of

$$\det(\boldsymbol{S}^{\text{tot}} - \boldsymbol{G}) = 0, \tag{4}$$

which is a function of both the amplitude and frequency of the wave variable $\boldsymbol{a}$. The steady state value, $\boldsymbol{a}_o$, is determined by solving (3) subject to the constraints given by (4). In other words, $\boldsymbol{a}_o$ spans the nullspace of $(\boldsymbol{S}^{\text{tot}} - \boldsymbol{G})$ when (3) obtains.

Since $\boldsymbol{S}^{\text{tot}}$ and $\boldsymbol{G}$ are 8×8 matrices, (4) has many terms. In the case of our oscillator, however, experimental data indicate that the reflection coefficient and reverse coupling of the coupler, and the reverse amplification of the FET amplifier are an order of magnitude smaller than the other elements of $\boldsymbol{S}^{\text{tot}}$. The same observation holds true for the reflection coefficient of the injection source. If we neglect these terms, (4) reduces to

$$1 - AC - \Gamma_i\Gamma_o C^2 - \Gamma_{\text{pat}}\Gamma_o T^2 = 0, \tag{5}$$

where A is the voltage gain of the FET amplifier, Γ_i and Γ_o are the input and output voltage reflection coefficients of the FET amplifier, C and T are the coupling and transmission coefficients of the microstrip directional coupler, and Γ_{pat} is the reflection coefficient of the patch antenna. Therefore, at steady state, the gain and phase of the amplifier must be given by

$$A = \frac{1 - \Gamma_i\Gamma_o C^2 - \Gamma_{\text{pat}}\Gamma_o T^2}{C}. \tag{6}$$

B. Injection Locking

To determine the injection locking bandwidth of the oscillator, we turn on the source and load generators shown in Fig. 1. In this case, (1) becomes

$$\boldsymbol{b} = \boldsymbol{S}^{\text{tot}}\boldsymbol{a} + \boldsymbol{c}, \tag{7}$$

where the ith element of the injection vector $\boldsymbol{c}$ is the amplitude of the wave impressed by the injection source at the ith port. Combining (7) and (2) gives

$$\boldsymbol{a} = (\boldsymbol{G} - \boldsymbol{S}^{\text{tot}})^{-1}\boldsymbol{c}. \tag{8}$$

For the circuit of Fig. 1, the injected signal may emanate from ports 7 and 8; the first six elements of $\boldsymbol{c}$ are zero.

To determine a simple expression for the small-signal injection locking range of the oscillator, we apply ap-

proximations to the solution of (8). The first step is to approximate the wave vector $\boldsymbol{a}$ under injection locked conditions by

$$\boldsymbol{a} = \boldsymbol{a}_o + \boldsymbol{G}^{-1}\boldsymbol{c} + \boldsymbol{G}^{-1}\boldsymbol{S}^{\text{tot}}\boldsymbol{G}^{-1}\boldsymbol{c}.$$

The first term on the right hand side is the free-running solution, the second term is the injection vector expressed as an incident wave at ports 1 and 4, and the third term accounts for the propagation of the injected signal through the coupler. When this expression is substituted into (8), neglecting terms of second order, the result is

$$a_3 = \frac{c_7 T(A + \Gamma_i\Gamma_o C + \Gamma_{\text{pat}}\Gamma_o C) + c_8\Gamma_o T}{\Delta}, \quad (9a)$$

where

$$\Delta = \text{Det}\,(\boldsymbol{G} - \boldsymbol{S}^{\text{tot}}) = 1 - AC - \Gamma_i\Gamma_o C^2 - \Gamma_{\text{pat}}\Gamma_o T^2, \quad (9b)$$

and c_7 and c_8 are the injection waves emanating from ports 7 and 8. This expression is recognized as the gain of a feedback amplifier, where effects due to component mismatch are accounted for by additional terms in Δ.

An expression for the locking bandwidth is first derived for the case where $\Gamma_i = \Gamma_o = \Gamma_{\text{pat}} = 0$, with a single injection source at port 1, ($c_8 = 0$). The more complicated case is discussed afterwards. To begin, we re-write (9) as

$$a_3 = ATc_7 + ACa_3 \quad (10)$$

noting that $|c_7\text{AT}| \ll |a_3|$ and $|\text{AC}| \approx 1$. Equation (10) is represented by the phasor diagram in Fig. 2, where θ represents the angle between $\text{AC}a_3$ and a_3, and ϕ represents the phase angle between $\text{AT}c_7$ and $\text{AC}a_3$. The extrema of the injection locking range occur when $\phi = \pm\pi/2$. At these points, the corresponding values for θ are

$$\theta_{\min} = -\frac{|c_7 AT|}{|a_3|} \text{ and } \theta_{\max} = +\frac{|c_7 AT|}{|a_3|}, \quad (11)$$

where we use the small argument approximation for $\sin\theta$.

We now make the additional assumption that the phase angles of the circuit parameters A, C, and T vary linearly over the locking range, while their magnetics remain constant. Measurements indicate that this approximation is quite reasonable for bandwidths of a few percent . If we let $|\theta_{\min}| = |\theta_{\max}| = \Delta\theta$, and note that this is equal to the changes in phase angle of AC over half the locking range, we get

$$\Delta\theta = \frac{d}{d\omega}(\angle AC)\,\Delta\omega \equiv B\,\Delta\omega = \frac{|c_7 AT|}{|a_3|}, \quad (12)$$

where $\Delta\omega$ is one half of the injection locking bandwidth, and B is the rate of change of phase of AC at the center frequency. We may re-write (12) in terms of the input and output signals of the oscillator, substituting $|A| = 1/|C|$, $|a_3| \cdot |T| = |a_o|$, and $|c_7| = |a_i|$, to get

$$\Delta\omega = \frac{|T|^2}{B|C|} \cdot \frac{|a_i|}{|a_o|} \quad (13)$$

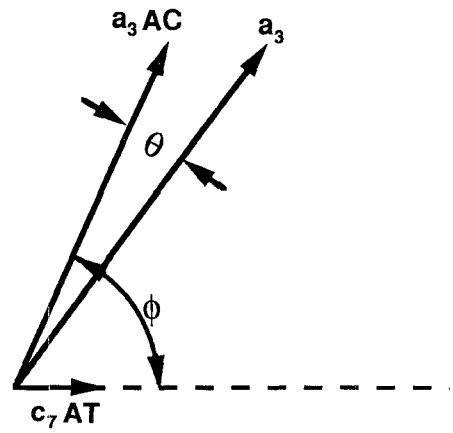

Fig. 2. Phase relationship between signals in locked oscillator.

by comparison with Adler's result [12], we may define an effective Q for the feedback oscillator as

$$Q_{\text{eff}} = \frac{B|C|\omega_0}{2|T|^2}, \quad (14)$$

where ω_0 is the center of the injection locking range. For the FET oscillators used in the array, $Q_{\text{eff}} \sim 1$. This low value indicates that the oscillator element exhibits a broad injection locking bandwidth.

For the case where the reflection coefficients of the amplifier and the patch are not zero, the additional terms in (9a) and (9b) may be carried in the above calculations, resulting in more complicated expressions in place of (13) and (14). The main effect will be the replacement of AC in (10) with $\Delta - 1$ from (9b). Since the difference between these two expressions is a sum of products of reflection coefficients, the latter may exhibit greater phase variation as a function of frequency. For well matched components, the difference is expected to be small.

C. Coupling Between Elements

Mutual coupling between the oscillator elements will have an effect on the injection locking behavior of the array. A qualitative explanation of the effects of this may be given with the aid of (9a).

Coupling between adjacent antennas in the array was measured at -15 dB. The coupling causes an unwanted injection signal to appear at the output port of each oscillator. The phase of this will vary rapidly with frequency when compared with the phase of the internal feedback signal in the oscillator, because of the large spacing between the patches. This results in rapid phase changes in c_8 in (9a). If $|c_8|$ is large enough, the effect will be the same as loops in the feedback transfer function [9]. Since $|c_8|$ is relatively constant for any value of the injection signal, it is expected that the effects of mutual coupling will be most pronounced at lower injection levels. This will be seen in the graph of locking bandwidth versus injected signal level.

III. Design and Construction

The oscillator elements described in the previous section were used to form a quasi-optical power combining array, where the output from each oscillator was fed to a separate patch antenna, and the resulting radiated fields combined in free space. The individual oscillator elements were synchronized in-phase by locking to a single external source using a network of cascaded Wilkinson power dividers. The array was constructed using a two sided microstrip structure, with a common ground plane in the center. The patch antennas were located on one side of the structure, while the oscillator elements and injection feed network were located on the opposite side. A drawing of an oscillator element appears in Fig. 3, and the top and side views of the array appear in Figs. 4 and 5.

The two sided structure was employed for several reasons. First, this structure allows for the use of dielectric materials and thicknesses suitable for the different needs of the oscillator circuitry and the patch antenna. The use of a low ϵ_r material on the antenna side provided for broad band operation of the patches. The oscillator circuits could then be fabricated on thin dielectric material which is better suited to circuit design. Additional reasons for using the two-sided approach are that it simplifies the circuit design and minimizes the area of the array.

A. The Oscillator Elements

The oscillator elements were designed using small signal linear techniques with the help of the Touchstone microwave CAD program from EEsof of Westlake Village, CA. The transistors used were small signal packaged GaAsFETs with an fmax of 60 GHz. Each transistor's scattering parameters were measured in the range of 4–8 GHz using a Hewlett Packard 8510 network analyzer and a TRL test fixture, and these data were used in the Touchstone analysis.

The circuit was designed for operation at a frequency of 6 GHz, using 0.79 mm thick glass reinforced PTFE circuit material with a relative dielectric constant of 2.55. The procedure used was to simulate the open loop performance of the FET amplifier in series with the microstrip directional coupler. Circuit parameters were then adjusted for zero phase shift and two to three dB of gain through the loop, and return loss of better than 12 dB at the input and output of the amplifier. Recent measurements in our laboratory have shown that the phase shift through a similar type of single FET amplifier does not vary greatly with the incident power level, indicating that the operating frequency predicted by small signal analysis should be relatively accurate for steady-state oscillation [13].

The circuit was designed for ease of tuning, to accomodate a group of transistors exhibiting a range of RF characteristics. The schematic view in Fig. 3 shows the two principle tuning elements: the length of the short circuit stub attached to the gate, and the length of the open circuit stub at the output of the amplifier. Using these tuning elements, the free-running frequency of a typical oscillator could be adjusted from 5.5 to 6.5 GHz. The FET's were

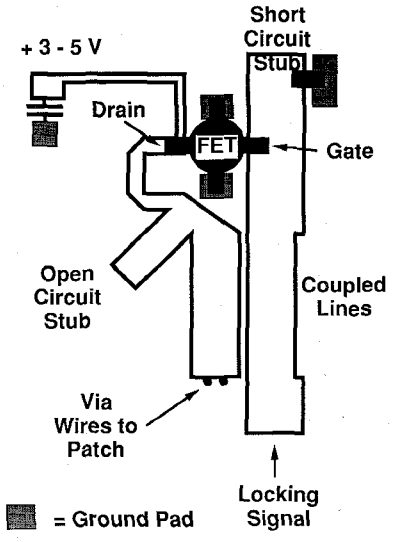

Fig. 3. Microstrip layout of the oscillator element.

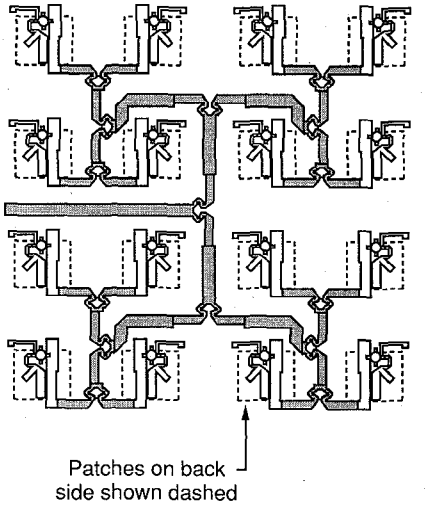

Fig. 4. The 16 element array.

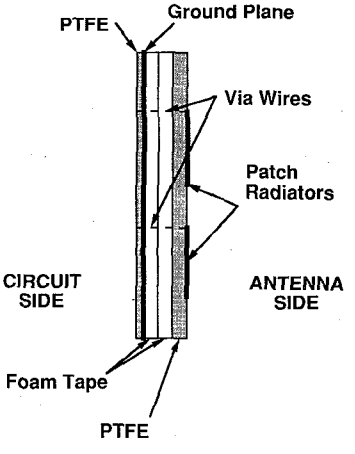

Fig. 5. Side view of the array, showing the layered structure.

biased at V_{ds} = 4.0 V and $I_d = I_{dss}$, which ranged from 35 to 45 mA. The output power for a typical oscillator was in the range of 7 to 14 dBm.

B. The Patch Radiators

The main criteria in the choice of a radiating element for this array were small size, broad VSWR bandwidth, and ease of construction. The layered structure shown in Fig. 5 satisfied these criteria.

The patch element was a rectangular piece of copper tape bonded to a 1.60 mm thick layer of woven glass reinforced PTFE material with $\epsilon_r = 2.55$. This was then attached to the ground plane using two layers of 1.60 mm thick double sided foam tape. The connection to the patch from the opposite side of the ground plane was made using two 0.635 mm diameter copper wires, approximately 5.6 mm long. The antenna dimensions were determined in an empirical fashion, using the 8510 network analyzer. The final dimensions used in the 16 element array were 17.3 × 18.8 mm. This antenna exhibited a 2:1 VSWR bandwidth of 840 MHz at a center frequency of 6.10 GHz, which is more than 13 percent.

C. The Array

The 16 element array is shown in Fig. 4. Spacing between the oscillator elements is 27.9 mm in the x and y directions. The overall dimensions of the substrate are 12.7 × 12.7 cm. The injection signal is distributed from a single input to the 16 oscillator elements using a cascade arrangement of 15 Wilkinson power dividers. For a single power divider, measured values for isolation between output ports and return loss were better than 20 dB at 6 GHz, with an insertion loss of less than 0.3 dB.

Since the FET's were biased at I_{DSS}, only one bias connection was necessary for each element. The bias leads were connected together so that all of the elements were fed from a single supply.

IV. Test and Results

Before measuring the array performance, the individual oscillators were tuned as close as possible to a common free-running frequency. It is necessary for the individual oscillators to have nearly identical oscillation frequencies and locking bandwidths for good array performance. This is because the phase shift between the injection and output signals varies by 180 degrees over the locking range for each oscillator. Table I shows results for the individual elements after tuning. (These data, and all those which follow, were measured in a small antenna range lined with microwave absorber, using a WR-137 waveguide flange in a ground plane at a range of 170 cm for the receive antenna.)

The array was operated by connecting the bias lines from the elements to a single supply, and using an HP sweep oscillator as the injection source. E and H plane patters for the array are shown in Fig. 6, where the FET's were biased at 4 V *Vds* and the array drew 540 mA. The low cross-polarized radiation levels and symmetry of the pattern indicate balanced operation of the elements.

TABLE I
Distribution of ERP, Free-Running Frequency, and Locking Range for the Individual Elements in the Array, at a Bias Voltage of 4 V

	Average	Minimum	Maximum	Standard Deviation
ERP, dBm	16.0	8.0	19.6	3.17
Free-running Frequency, GHz	6.04	5.98	6.13	0.044
Locking Range, MHz, for $P_{inj} = -12$ dBm	282	220	400	53.1

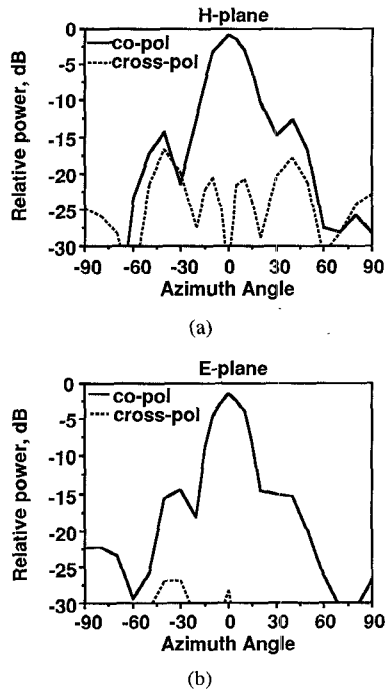

Fig. 6. Radiation patterns for the 16 element array: (a) H-plane. (b) E-plane.

The ERP and isotropic conversion gain (G_{iso}) for the array were measured by comparison with a Narda model 646 standard gain horn. The maximum ERP was measured at 28.2 W, with the array biased at 5 V and drawings 580 mA. Since G_{iso} is determined by dividing the ERP by the dc power to the array [14], this gives a G_{iso} of 9.9 dB.

The ERP for the array at 4 V bias was 16.6 W. If the data shown in Table I is used to calculate combining efficiency for the array, a value of more than 150% is given. The reason for this is two-fold: First, the data shown in Table I are for the free-running case, while the array ERP was measured in injection locked operation. Secondly, interaction between the oscillating elements alters the operating points of the oscillators, thereby affecting output power. In any event, the array demonstrates good power combination performance.

The phase between the injected and the output signals

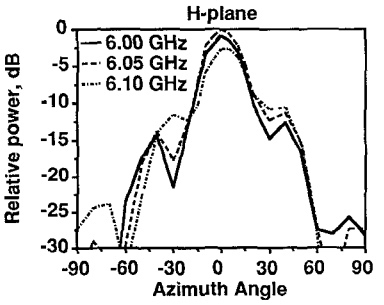

(a)

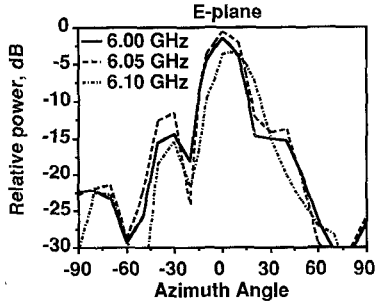

(b)

Fig. 7. Variation of radiation pattern with frequency: (a) H-plane. (b) E-plane.

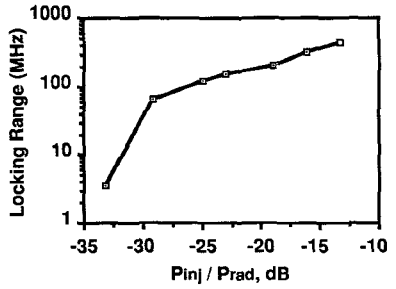

Fig. 8. Injection locking range as a function of the ratio of input to radiated power.

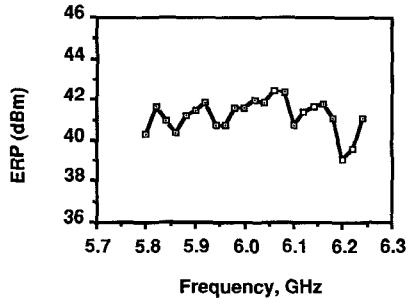

Fig. 9. Variation in ERP with injection frequency; injection level = 10.3 dBm.

to each oscillating element varies by more than 180 degrees over the locking range. If the free-running frequencies for the elements are not sufficiently close together, the phase of the output signals may vary a great deal from one antenna to the next, even though the elements are all locked to the same frequency. To investigate this possibility, antenna patterns were measured at the center and extrema of the locking frequency range for an injection signal level of 0 dBm into the feed network. The results, shown in Fig. 7, show that, aside from a variation in ERP, no serious pattern degradation occurs as a result of varying the locking frequency. The analysis given above indicates that non-uniformity of the phase shift through the individual elements should decrease as the injection level is arised.

The injection bandwidth for the array is shown in Fig. 8 as a function of injected signal power at the 4 V V_{DS}. In this figure, P_{rad} was calculated from the measured data using the theoretical array gain and the measured element gain of an individual patch. P_{inj} is the power measured at the input to the feed network. The reduction in locking bandwidth at low injection levels due to coupling between the oscillators is apparent. Variation in output power with locking frequency is shown in Fig. 9, for an injection signal level of 10.3 dBm.

V. Conclusion

A new approach to quasi-optical power combining has been discussed, which uses an array of two-port FET oscillator elements which are synchronized to a single external source. A Wilkinson power combining network distributes the injection signal to the individual oscillators, whose outputs are connected to patch radiators on the opposite side of a ground plane. This method provides for convenient injection locking of the array, which greatly enhances its usefulness. A simple analysis of the injection locking behavior of the oscillator elements has also been given.

It is important to discuss the application of monolithic techniques to the fabrication of this type of an array. One approach would be to construct individual dice consisting of a small number of oscillator elements, perhaps four. These dice would then be individually tested to insure uniform oscillation characteristics, and assembled along with a power dividing injection network and patch array into a structure similar to the prototype described above. This method may be contrasted with the quasi-optical arrays described in [3]–[8], which appear more suited to wafer-scale fabrication.

Finally, by removing the input feed network and adding a receive antenna to the input of each oscillator element, the array could be injection locked from a spatial feed. In such an array, the elements could be located according to the Fresnel zones of the feed source, thereby forming an active, injection locked zone plate for amplifying and focusing the injection signal.

VI. Acknowledgment

The authors would like to acknowledge many helpful discussions with H. Foltz regarding injection locking.

VII. References

[1] K. Chang and C. Sun, "Millimeter-wave power combining techniques," *IEEE Trans. Microwave Theory Tech.*, vol. MTT-31, pp. 91–107, Feb. 1983.

[2] J. W. Mink, "Quasi-optical power combining of solid-state millimeter-wave sources," *IEEE Trans. Microwave Theory Tech.*, vol. MTT-34, pp. 273–279, Feb. 1986.

[3] K. D. Stephan, "Inter-injection-locked oscillators for power combin-

ing and phased arrays," *IEEE Trans. Microwave Theory. Tech.*, vol. MTT-34, pp. 1017–1025, 1986.
[4] N. Camilleri and B. Bayraktaroglu, "Monolithic mm-wave IMPATT oscillator and active antenna," *IEEE Trans. Microwave Theory Tech.*, vol. 36, pp. 1670–1676, Dec. 1989.
[5] K. Chang, K. A. Hummer, and J. L. Klein, "Experiments on injection-locking of active antenna elements for active phase arrays and spatial power combiners," *IEEE Trans. Microwave Theory Tech.*, vol. 37, pp. 1078–1084, July 1989.
[6] R. A. York and R. C. Compton, "A 4 × 4 array using Gunn diodes," in *1990 IEEE AP-S Int. Symp. Dig.*, Dallas, TX, May 1990, pp. 1146–1149.
[7] J. Birkeland and T. Itoh, "Spatial power combining using push-pull FET oscillators with microstrip patch resonators," in *1990 IEEE MTT-S Int. Microwave Symp. Dig.*, Dallas, TX, May, 1990, pp. 1217–1220.
[8] Z. B. Popovic, R. M. Weikle, M. Kim, and D. B. Rutledge, "A 100 MESFET planar grid oscillator," *IEEE Trans. Microwave Theory Tech.*, vol. 39, Feb. 1991, pp. 193–200.
[9] K. Kurokawa, "Injection locking of microwave solid-state oscillators," *Proc. IEEE*, vol. 61, no. 10, pp. 1386–1410, Oct. 1973.
[10] J. Birkeland and T. Itoh, "Two port FET oscillators with applications to active arrays," *IEEE Trans. Microwave Guided Wave Lett.*, vol. 1, no. 5, pp.112–113, May 1991.
[11] K. C. Gupta, R. Garg, and R. Chadha, *Computer Aided Design of Microwave Circuits*, Dedham, MA: Artech House, 1981, ch. 11, p. 338.
[12] R. Adler, "A study of locking phenomena in oscillators," *Proc. IRE*, vol. 34, pp. 351–357, June 1946, reprinted in *Proc. IEEE*, vol. 61, no. 10, pp. 1380–1385, Oct. 1973.
[13] J. Birkeland and T. Itoh, "A circularly polarized FET oscillator active radiating element," in *1991 IEEE MTT-S Int. Microwave Symp. Dig.*, Boston, MA, June 1991, pp. 1265–1268.
[14] ——, "FET-based planar circuits for quasi-optical sources and transceivers," *IEEE Trans. Microwave Theory Tech.*, vol. 37, no. 9, pp. 1452–1459, Sept. 1989.

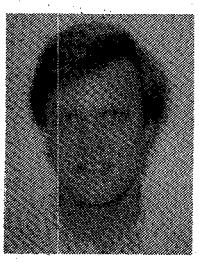

Joel Birkeland (S'87–M'89) received the B.S. degree in physics from Oregon State University in 1982, the M.S.E. degree in electrical engineering from Arizona State University in 1985, and the Ph.D. degree in electrical engineering from The University of Texas at Austin in 1989.

From February 1985 to August 1987 he was employed at M/A-COM Active Assemblies Division in Tempe, AZ, where he worked on low noise microwave amplifiers. From September 1989 until May 1991 he was with The University of Texas at Austin, where he was a Post-Doctoral Fellow. In July 1991 he began work for Motorola Semiconductor Products Sector in Tempe, AZ. His interests lie in the area of solid state microwave circuit design.

Dr. Birkeland was the recipient of an MTT-S fellowship for 1989.

Tatsuo Itoh (S'69–M'69–SM'74–F'82) received the Ph.D. degree in electrical engineering from the University of Illinois, Urbana in 1969.

From September 1966 to April 1976, he was with the Electrical Engineering Department, University of Illinois. From April 1976 to August 1977, he was a Senior Research Engineer in the Radio Physics Laboratory, SRI International, Menlo Park, CA. From August 1977 to June 1978, he was an Associate Professor at the University of Kentucky, Lexington. In July 1978, he joined the faculty at the Univesity of Texas at Austin where he became a Professor of Electrical Engineering in 1981 and Director of the Electrical Engineering Research Laboratory in 1984. During the summer of 1979, he was a guest researcher at AEG-Telefunken, Ulm, West Germany. In September 1983, he was selected to the Hayden Head Centennial Professorship of Engineering at The University of Texas. In September 1984, he was appointed Associate Chairman for Research and Planning of the Electrical and Computer Engineering Department at The University of Texas. In January 1991, he joined the University of California, Los Angeles as Professor of Electrical Engineering and holder of the TRW Endowed Chair in Microwave and Millimeter Wave Electronics.

Dr. Itoh is a member of the Institute of Electronics and Communication Engineers of Japan, Sigma Xi, and Commissions B and D of USNC/URSI. He served as the Editor of IEEE TRANSACTIONS ON MICROWAVE THEORY AND TECHNIQUES 1983–1985. He serves on the Administrative Committee of IEEE Microwave Theory and Techniques Society. He was Vice President of the Microwave Theory and Techniques Society in 1989 and President in 1990. He is the Editor-in-Chief of IEEE Microwave and Guided Wave Letters. He was the Chairman of USNC/URSI Commission D from 1988 to 1990 and is the Vice Chairman of Commission D of the Interational URSI.